

Numerical study of shear-strengthened post-tensioned concrete girders using externally bonded CFRP laminates

Yousef A.Ahmed¹, Ayman H.Khalil² and Ezz El-Deen Mostafa³

¹Teaching Assistant of Structural Engineering, Cairo, Egypt.

²Professor of Reinforced Concrete Structures, Structural Engineering Department, Ain Shams University, Cairo, Egypt.

³Lecturer of Reinforced Concrete Structures, Structural Engineering Department, Ain Shams University, Cairo, Egypt.

Corresponding Author: Yousef Amr Ahmed Amin

Abstract: Using nonlinear Finite-Element-Method (FEM), a three-dimensional model is built for post-tensioned (PT) concrete girders that are strengthened in shear using externally bonded (EB) carbon Fibre-Reinforced-Polymer (CFRP) reinforcement. The finite element (FE) model for a control/reference T-section girder was validated using experimental work that is found in the literature. A parametric study was executed to investigate the effectiveness of EB CFRP strengthening, different configuration scheme of CFRP laminates and configuration of orientation angle on the predicted shear force capacity of the aged/damaged girders. The outputs of the study exhibited that shear strengthening with EB CFRP could be an effective tool for enhancement of the shear capacity of (PT) concrete girders.

Keywords: Finite element; Pre-stressed concrete; Post-tensioned concrete; Girders; Shear; Strengthening; Fibre reinforced polymer.

Date of Submission: 10-12-2022

Date of Acceptance: 24-12-2022

I. Introduction

Pre-stressed concrete beams have been widely used in construction, especially for bridge girders; when the bridge is subjected to cyclically overloaded traffic, poor initial design, internal steel corrosion, tough exposure conditions, and structural retrogradation due to ageing, so that such structural members are needed to be maintained and strengthened (1,2).

Over the past three decades, FRPs composite materials have been used in construction. Traditional steel reinforcement can be swapped out for FRP composites in new construction due to its light weight, high tensile strength to weight ratio and anti-corrosive properties. For the strengthening, rehabilitation, and repair of ageing and damaged structures, externally bonded composite plates and/or sheets are used for preference of its ease to handle and install on different irregular surfaces and low cost viable solution because of the reduction of construction time compared to conventional methods, so that; the different applications of FRP strengthening holds the most promise as a financially sensible solution to the issue of structurally deficient concrete structures (3–5). Recently, various researches were performed in literature to study the performance of the EB technique that is applied for shear deficit pre-stressed concrete girders (6–8).

Regarding that area of interest in strengthening pre-stressed concrete girders, most of the research is carried out by scaled experimental programs that focused on verifying the effectiveness of the strengthening technique used, while using FEM such a powerful tool to perform computational simulations is not much around. The physical and/or numerical simulations provides inferential results on the performance of the pre-stressed concrete girders and the local behavior of constitutive materials. Furthermore, the production of full-scale specimens that costs a lot to be examined often straitens the evaluation of the various parameters that influence the shear behavior of the strengthened pre-stressed concrete girders (9).

Many commercial software packages using FE analysis are available to simulate and analyze the different concrete elements. In this paper ABAQUS software by Dassault Systemes Simulia Corporation (10) is used to investigate the parametric study of the CFRP shear strengthened PT concrete girder. The numerical model is validated first using experimental outputs that is found in the literature (11). Subsequently, the validated model will be used to investigate the effectiveness of EB CFRP strengthening, different configuration scheme of CFRP laminates and configuration of orientation angle on the predicted shear force capacity of the PT girders.

II. Brief of the experimental work

In this paper work, the FE model is validated with the experimental study which conducted by P. Huber et al. (11). They conducted a three-point laboratory test on T-section post-tensioned concrete specimen

labelled (PC4.5T168e) that is shown in Figure (1). The unstrengthened validated girder will be assigned as a control beam for our parametric study after.

The compressive cylinder strength (f_{ck}) was equal to 69.3 MPa, with 32.927 GPa modulus of elasticity and 4.5 MPa splitting tensile strength (f_{ct}). The mechanical properties and layout of reinforcing steel and pre-stressing steel are shown in Table (1) and Figure (2). The pre-stressing process needed one tendon consists of 7-wire strands with area equals to 1050 mm², the strands are type Y1860S7-15.7 with young's modulus equals to 198 GPa. The tendon was initially pre-stressed to 1066 MPa approximately.

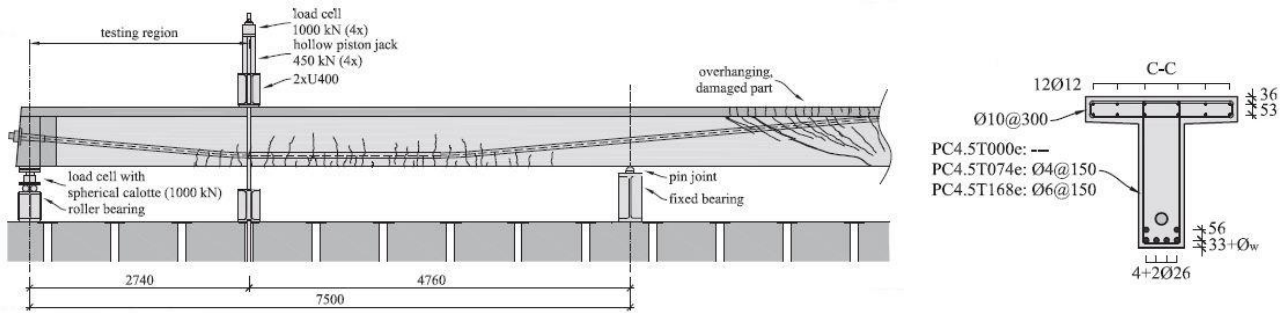


Figure (1): PC4.5T168e specimen test set-up

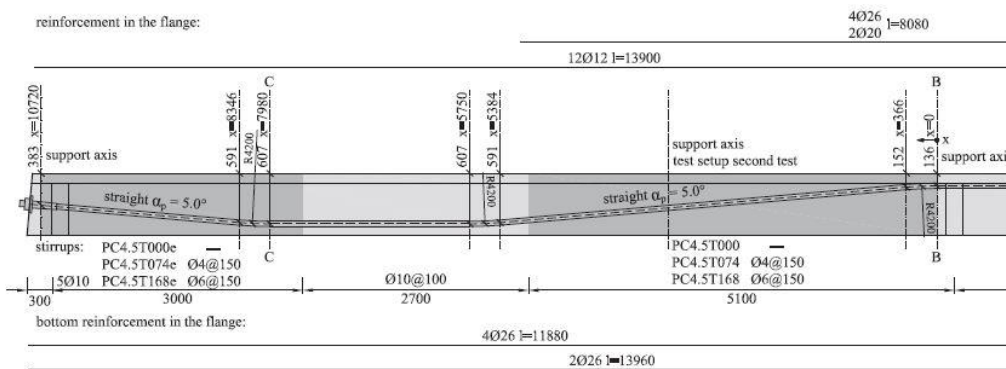


Figure (2): Layout of the reinforcement steel and tendon profile

Mechanical properties of the reinforcing and prestressing steel.

Reinforcing/ prestressing steel	Type	Ø [mm]	$f_{y,0.1}$	$f_{y,0.2}$	f_t [MPa]	A_{gr} [%]
Reinforcing steel	Cold-worked	4		651	691	4.2
Reinforcing steel	Cold-worked	6		511	588	4.2
Reinforcing steel	Hot-rolled	20		598	686	8.7
Reinforcing steel	Hot-rolled	26		562	657	8.5
Prestressing steel	7-Wire strand	15.7	1750	1781	1908	4.4

Table (1): Reinforcing and pre-stressing steel mechanical properties

III. Finite element modelling

A three-dimensional FE model is built using ABAQUS(10) to simulate the conducted experimental test, but due to the un-symmetry of test specimen in the longitudinal direction the girder is simulated with its full-scale which causes more computational time. Constitutive models and elements types that are used in the FE model will be briefly discussed in the following subsections:

Concrete behavior

A deformable, homogenous solid part was created, assigning a three-dimensional, 8-node, first-order hexahedral continuum element type (C3D8R) and approximate element size equals to 30 mm which exhibited the preferable predictions. Reduced integration and hourglass control were adopted.

(BS EN1992-1-1) (12) formulation is used to express the non-linear plastic behavior of concrete material under uniaxial compression as presented in Figure (3). Where ϵ_{cu1} is the nominal ultimate strain, while ϵ_{c1} is the corresponding strain to the peak stress value f_{cm} , (knowing that $f_{cm} = f_{ck} + 8$ (inMPa)).

While the uniaxial tensile behavior of concrete is assumed linear till catching up the cracking stress value, i.e. modulus of rupture. Beyond the modulus of rupture, P. Kmiecik and M. Kamiński (13) have proposed a modified Wang & Hsu (14) formula which describes the behavior of concrete in tension stiffening zone.

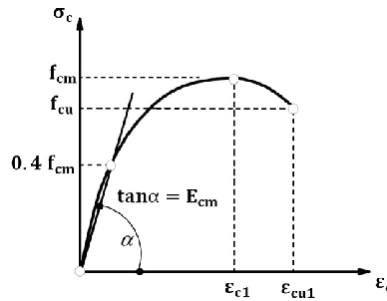


Figure (3): Compressive stress-strain diagram of concrete according to Eurocode2

Loading, supporting plates and anchor block

Loading, supporting plates and anchor blocks are used to preclude stress concentration in concrete elements which may cause convergence issues. The same as concrete element type, they were created using a deformable, homogenous solid parts, assigning a three-dimensional, 8-node, first-order hexahedral continuum element type (C3D8R) with reduced integration, hourglass control and approximate element size equals to 30 mm. They are assumed to have a behavior of a linear elastic material with high modulus of elasticity equals to 300 GPa.

Reinforcement steel and tendon

All reinforcement steel is created using a deformable, wire parts which were discretized by using a three dimensional, 2-node, first-order truss elements (T3D2), with reduced integration, hourglass control and approximate element size equals to 30 mm. The different types of bars which are presented in Table (1), were assumed to have a bilinear elastic-plastic behavior with poisson's ratio equals to 0.3.

On the other hand, tendon is created using a deformable, homogenous solid part, assigning a three-dimensional, 6-node, first-order triangular prism element type (C3D6), with reduced integration, hourglass control and approximate element size equals to 30 mm. It was assumed to have a linear behavior up to its yielding point, while the developed power formula which has been presented by Devalapura and Tadros(15) is used to model the non-linearity of pre-stressing steel behavior for steel grade 270 ksi seven-wire strand.

CFRP laminates

For CFRP laminates, a deformable, shell part was created, assigning a three-dimensional, 4-node shell element type (S4R) with approximate element size equals to 30 mm. Reduced integration and hourglass control were used.

The used CFRP laminates come in a single ply with 0.11 mm effective thickness, while the ultimate tensile stress (i.e., rupture strength) is 3450 MPa with modulus of elasticity equals to 230 GPa and an ultimate elongation equals to 1.5%. The tensile behavior of the CFRP laminates was considered to be unidirectional linear elastic up to the ultimate stress, while the contribution gained after this point is assumed to be ignored.

Interface between CFRP and concrete

A bi-linear triangular bond slip model (i.e., traction separation law) shown in Figure (4) which was developed by Yuichi Sato and Frank J. Vecchio (16), is used for modelling the interface between the CFRP and concrete using surface-to-surface discretization. Because concrete's top surface layer is usually weaker than the adhesive layer itself, the model assumes that bond failure takes place through the surface layer of concrete which is adjacent to adhesive-to-concrete interface.

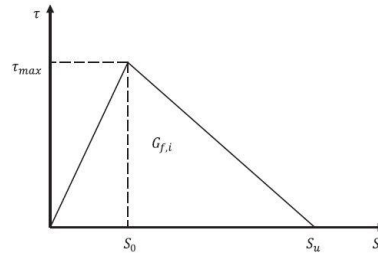


Figure (4): Bi-linear bond slip model used in Abaqus

Where τ_{max} , s_0 are the peak bonding stress and the corresponding slip (i.e. displacement) which refers to debonding initiation. While s_u is the maximum slippage value which refers to the limit of a complete debonding, and $G_{f,i}$ is the area under the curve of traction separation law which is defined by the interfacial fracture energy.

Boundary conditions and loading application

The boundary conditions that assigned to the PT concrete girder are modelled as the experimental work in laboratory. The interior right supporting plate is constrained from the all three directional translations (3 rotational degrees of freedom only) representing the hinged support, while the end left one is constrained form Y-direction translation (five degrees of freedom) representing the roller support.

The loading test in Abaqus was typically carried out under displacement control mode by adding a translation constraint in Y-direction (2-direction U2) with the final displacement value of the PT beam that would be achieved, leading to more stable behavior of the test specimen.

IV. Validation work

The numerical result of the FE model which is labelled (PT-0.0) was validated by mean of comparing it with the results of the experimental work of the test specimen (PC4.5T168e) in terms of shear force-displacement curve which is presented inFigure (5), and failure criteria of compressive failure mode pattern (DAMAGEC) in ABAQUS which is shown inFigure (6).

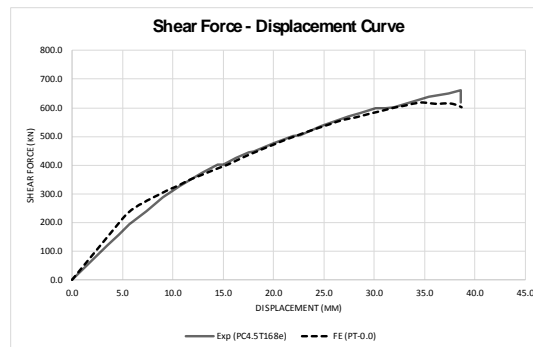


Figure (5): Shear force-displacement curve for (PC4.5T168e) test specimen

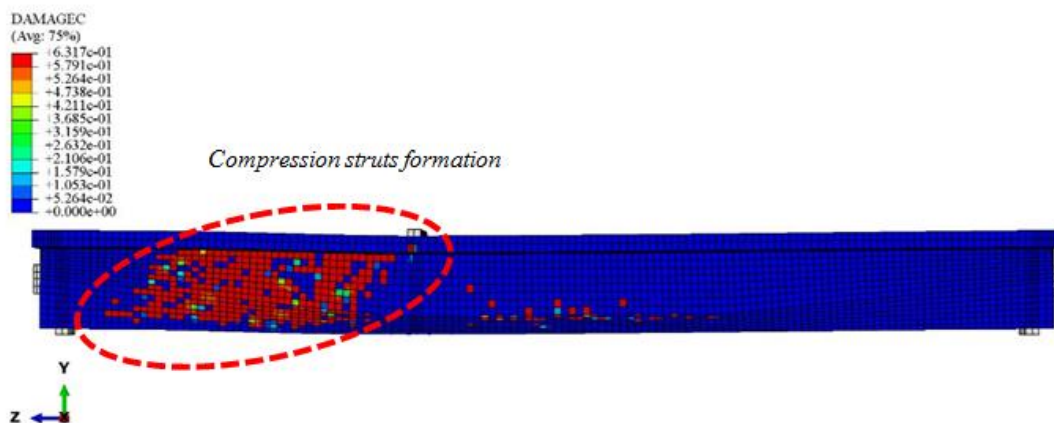


Figure (6): Compressive damage failure mode of (PC4.5T168e) test specimen

V. Parametric study

A total of three FE models of shear strengthened PT Concrete girders using CFRP laminates along the shear span that are presented in Table (2), have been carried out to study and measure the performance of the parameters that are influencing the shear capacities of the shear deficit girders. The first strengthened girder that is labelled (PT-S90⁰) is strengthened using unidirectional CFRP straight strips which are making 90⁰ configuration angle with the longitudinal axis of the girder, the strips are EB only on the two sides of the girder. The Strips of the second strengthened one that is labelled (PT-I45⁰) are inclined strips with 45⁰ configuration angle, and EB only on the two sides of the girder too. While the third one which is labelled (PT-U90⁰) is strengthened using unidirectional CFRP straight strips with 90⁰ configuration angle and U-jacket configuration scheme. The all three models are sharing the same rigidity of CFRP material with strip width (W_f) which is equals to 60mm, and 123mm strip spacing (S_f).

All FE models failed in shear, and in order to investigate the effect of the parameters, all models had the same geometry and material properties of the validated control girder that labelled (PT-0.0).

Specimen Label	FRP Type	FRP Configuration	W _f (mm)	S _f (mm)	Orientation Angle ⁰
PT-0.0	—	—	—	—	—
PT-S90 ⁰	Carbon	Straight Sides	60	123	90 ⁰
PT-I45 ⁰	Carbon	Inclined Sides	60	123	45 ⁰
PT-U90 ⁰	Carbon	U-jacket	60	123	90 ⁰

Table (2): CFRP configuration details of the FE models

The following sub-sections will present the result of the studied parameters which are: 1) the effectiveness of EB CFRP strengthening on shear capacity of the PT concrete girders; 2) the effect of orientation angles configuration on the contribution of the CFRP in shear; 3) the effect of different configuration scheme of CFRP laminates on the contribution of the CFRP in shear.

Effectiveness of EB CFRP strengthening

The results of the three models of shear strengthened PT Concrete girders showed an increase in shear capacity due to the contribution of CFRP laminates. While the control girder (PT-0.0) was failed in shear at 619.48 KN shear force by means of concrete and internal steel terms only, the CFRP shear strengthened girders (PT-S90⁰), (PT-I45⁰) and (PT-U90⁰) have exhibited an improvement in shear capacity with respect to the control girder by 9%, 10.34% and 11% respectively. As noted, the results of shear enhancement for the three strengthened models are close because of using the same rigidity of CFRP. Figure (7) shows a bar graph of the increased shear force owing to CFRP laminates for the three models.

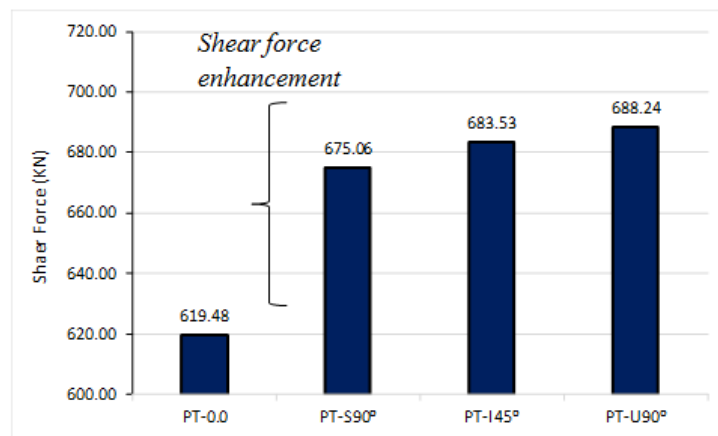


Figure (7): Shear force bar graph of the three models

Orientation angel

In order to measure the effect of the orientation angle of CFRP on shear contribution, same rigidity of the strengthening material has been used. The result of the (PT-I45⁰) model which had inclined strips with 45⁰ configuration angle, showed a better performance in ultimate shear force combined with a ductile manner than the (PT-S90⁰) model that had straight strips with 90⁰ configuration angle as shown in Figure (8). This could be attributed to the fact that the web shear crack in slender concrete girders propagates almost at angle 45⁰ due to diagonal tension and even more flatter in pre-stressed concrete girders due to the effect of the pre-stressing force, so the value of the effective strain induced in the inclined strips will be higher due to the orthogonal manner, exhibiting higher contribution than the vertical ones.

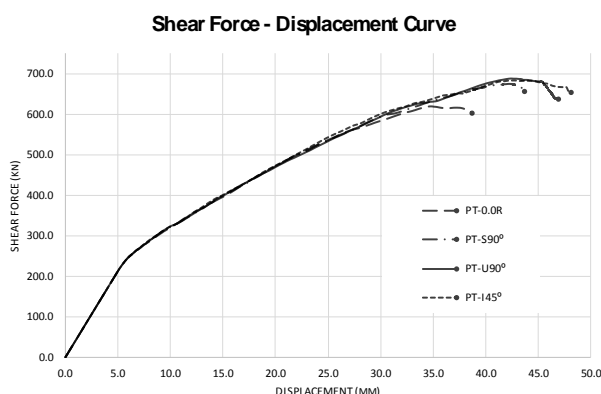


Figure (8): Shear force-displacement curve for the strengthened

Configuration scheme

Same rigidity of the strengthening material has been used for the two models (PT-S90⁰) and (PT-U90⁰) which were strengthened using EB sided strips and U-jacket configuration scheme respectively, in order to investigate the effect of different configuration scheme of CFRP on shear contribution. The result of the (PT-U90⁰) model exhibited a higher contribution in ultimate shear force than the (PT-S90⁰) model as shown in Figure (8). This result could be explained by the fact that the U-jacket configuration scheme laminates provides a reasonable anchorage length compared with the sided strips only.

VI. Conclusion

A numerical parametric study on shear deficit T-sectioned, post-tensioned (PT) concrete girders, has been conducted using nonlinear Finite-Element-Method to investigate the effectiveness of using small rigidity of carbon Fibre-Reinforced-Polymer (CFRP) on the contribution of shear capacity of (PT) concrete girders, and the induced outputs were as following:

1. The results of all models exhibited an improvement in shear capacity due to the contribution of CFRP laminates.
2. Using same rigidity of CFRP strengthening material led to a rapprochement in the ultimate shear force.
3. Using inclined strips with 45⁰ configuration angle, showed a better performance in ultimate shear force combined with a ductile manner than straight strips with 90⁰ configuration angle.
4. Using laminates with U-jacket configuration scheme exhibited a higher contribution in ultimate shear force than externally bonded sided strips only.

References

- [1]. Petty DA, Barr PJ, Osborn GP, Halling MW, Brackus TR. Carbon Fiber Shear Retrofit of Forty-Two-Year-Old AASHTO I-Shaped Girders. *J Compos Constr.* 2011;15(5):773–81.
- [2]. Valerio P, Ibell TJ, Darby AP. Deep embedment of FRP for concrete shear strengthening. *Proc Inst Civ Eng Struct Build.* 2009;162(5):311–21.
- [3]. Evans JT. Analysis and performance of fiber composites (second edition). Vol. 151, *Materials Science and Engineering: A.* 1992. 115 p.
- [4]. King RL. Fibre-reinforced composites materials, manufacturing and design. Vol. 20, *Composites.* 1989. 172–173 p.
- [5]. GangaRao HVS, Taly N, Vijay P V. Reinforced concrete design with FRP composites. *Reinforced Concrete Design with FRP Composites.* 2006. 1–382 p.
- [6]. Kang THK, Ary MI. Shear-strengthening of reinforced & prestressed concrete beams using FRP: Part II - Experimental investigation. *Int J Concr Struct Mater.* 2012;6(1):49–57.
- [7]. Murphy M, Belarbi A, Bae S. Michael Murphy, Abdeldjelil Belarbi, and Sang-Wook Bae. 2012;
- [8]. Thi Thu Dung NGUYEN, MATSUMOTO K, SATO Y, YAMADA M, NIWA J. Shear-Resisting Mechanisms of Pre-Tensioned Pc Beams Without Shear Reinforcement Strengthened By Cfrp Sheets. *J JSCE.* 2016;4(1):59–71.

- [9]. Dirar S, Lees JM, Morley C. Phased Nonlinear Finite-Element Analysis of Precracked RC T-Beams Repaired in Shear with CFRP Sheets. *J Compos Constr.* 2013;17(4):476–87.
- [10]. Corp DSS. *Abaqus Analysis User's Guide* 6.13.
- [11]. Huber P, Huber T, Kollegger J. Influence of loading conditions on the shear capacity of post-tensioned beams with low shear reinforcement ratios. *Eng Struct [Internet].* 2018;170(May):91–102. Available from: <https://doi.org/10.1016/j.engstruct.2018.05.079>
- [12]. Union TE. EN 1992-1-1. 2004.
- [13]. Kmiecik P, Kamiński M. Modelling of reinforced concrete structures and composite structures with concrete strength degradation taken into consideration. *Arch Civ Mech Eng.* 2011;11(3):623–36.
- [14]. Wang T, Hsu TTC. Nonlinear finite element analysis of concrete structures using new constitutive models. *Comput Struct.* 2001;79(32):2781–91.
- [15]. Devalapura RK, Tadros M. Stress-Strain Modeling of Prestressing Strands. *PCI J.* 1992;9(37(2)):100–6.
- [16]. Sato Y, Vecchio FJ. Tension Stiffening and Crack Formation in Reinforced Concrete Members with Fiber-Reinforced Polymer Sheets. *J Struct Eng.* 2003;129(6):717–24.

Yousef Amr Ahmed Amin, et. al. "Numerical study of shear-strengthened post-tensioned concrete girders using externally bonded CFRP laminates". *IOSR Journal of Mechanical and Civil Engineering (IOSR-JMCE)*, 19(6), 2022, pp. 57-63.